GOOGLE EARTH ENGINE BASED APPROACH FOR COASTAL WATER MONITORING: A CASE STUDY OF THE SOUTHERN SHORE OF CASPIAN SEA

S. Karimzadeh [1]*

[1] Dept. of Earth science, Faculty of science, Shiraz University, Iran- Karimzadeh-shu@shirazu.ac.ir

Commission IV, WG IV/3

KEY WORDS: Landsat 9 OLI, Landsat 5 TM, Shoreline change, Sea surface salinity, Logical operation algorithm, Mazandaran coastline, Monsoon

ABSTRACT:

Coastal regions are important, sensitive ecological systems and are also significant from an economic point of view as they are used for tourism, fishing, aquaculture, and recreation. An attempt was made to focus on the Caspian Sea including the southern shore of it, Mazandaran province, Iran using the Google earth engine platform. This study for the first time assesses the shoreline changes over 33 years and sea surface salinity, by using Landsat 5 TM and Landsat 9 OLI data acquired from the coastal region of the southern Caspian Sea. The coastal zone features were delineated using Landsat 5 TM and Landsat 9 OLI data respectively from 1988 and 2022. A manual identification technique was used for coastline extraction and detection. The advances in shoreline position were mainly detected over these 33 years in 6 points, as a result of breakwaters which are constructed to prevent erosion and the structural buildings such as recreational piers or wharves. The SSS expression was implemented on the datasets of pre-monsoon and post-monsoon seasons. The estimated SSS was in the range of 3-20 PSU. The higher range of SSS was spatially along the nearshore with a maximum of about 9-20 PSU in the pre-monsoon image. The SSS derived from the post-monsoon dataset illustrated a lower amount of SSS in some places nearshore which was due to the mixing of freshwater from river discharge and Indian monsoon precipitation in summer 2022. The obtained SSS was validated by in-situ measurement in 20 stations and the R^2 value of 0.92 showed a strong correlation between observed and satellite-derived SSS products.

1. INTRODUCTION

Coastal areas are significant and sensitive ecological systems, and are also economically important because they are used for aquaculture, fishing, tourism and recreation (Dassenakis et al., 2011). Different types of pollution such as physical, chemical, biological, or thermal can cause unfavourable effects to the marine environment, ecological harm, and even public health risk. Recent advances in the development of satellite data, image processing techniques, marine data collection techniques, and remote sensing modelling have provided powerful tools for analysing and monitoring ocean parameters (Palacios et al., 2009; Qing et al., 2013). In this research, an attempt was made to focus on the Caspian Sea including southern shore of it, even though there is limited research in this marine area. This study assesses the shoreline changes over about 30 years and sea surface salinity (SSS), by using Landsat 5 TM and Landsat 9 OLI data acquired from the coastal region of the southern Caspian Sea, Mazandaran province, Iran on Google Earth Engine (GEE) platform. The Web-based GEE enables easy access to satellite images and image processing. Mutanga and Kumar (2019) stated that the GEE platform is a great step in solving environmental problems affecting the earth because it has the power to manage huge data sets at different scales and build automated programs. Caspian Sea coastline changes in Mazandaran province was monitored years ago by Rasuly et al. (2010). However, this is the first study that measures SSS in this area using satellite data. Especially, this study has been focused on the effect of summer monsoon 2022 on Caspian Sea salinity by comparing the SSS before and after monsoon season. The summer monsoon is associated with heavy rainfall (Webster et al., 1998). Indian sub-continent summer monsoons usually bring some rain showers to Iran's arid plateau, but every few decades the impact becomes more intense and causes flooding (Webster et al., 1998; Jin et al., 2021). This year (2022) the Indian monsoon had above-average intensity over Iran during late July and early August.

2. MATERIALS AND METHODS

2.1 Study area

The southern shore of the Caspian Sea extends about 820 km through the Golestan, Mazandaran and Guilan provinces in Iran. The southern Caspian region has a subtropical climate (Alizadeh et al., 2018) and the rainfall gradually increases from the eastern coasts towards the west (Khaleghizavareh, 2005; Alizadeh et al., 2018). The study area is located in Mazandaran province, which includes the longest coastline (487 km) with respect to the other coastal provinces (Figure 1). Six Landsat data frame can cover the region of interest.

2.2 Satellite data

The median of Landsat 9 OLI (2022) and Landsat 5 TM (1988) data frames were provided for the southern shores of the Caspian Sea from GEE (Table 1). The Median of Landsat 9 OLI data were collected for two ranges of time pre- and post-monsoon (i.e., 2022-05-1 to 2022-06-31 and 2022-07-1 to 2022-08-31). The collected data had less than 6% cloud over the

* Corresponding author

entire scene. Each OLI and TM data were subset to the region of interest accordingly (Figure 2).

Figure 1. Google earth map of the southern shores of the Caspian Sea; red line shows the province boarder of Mazandaran.

Satellite data	Spatial resolution	Year	Purpose
Landsat 5 TM	60 m	1988	Detection of shoreline changes
Landsat 9 OLI	30 m	2022 (Pre-monsoon)	Detection of shoreline changes and Identifying the sea surface salinity
Landsat 9 OLI	30 m	2022 (Post-monsoon)	Identifying the sea surface salinity

Table 1. Description of the applied satellite data.

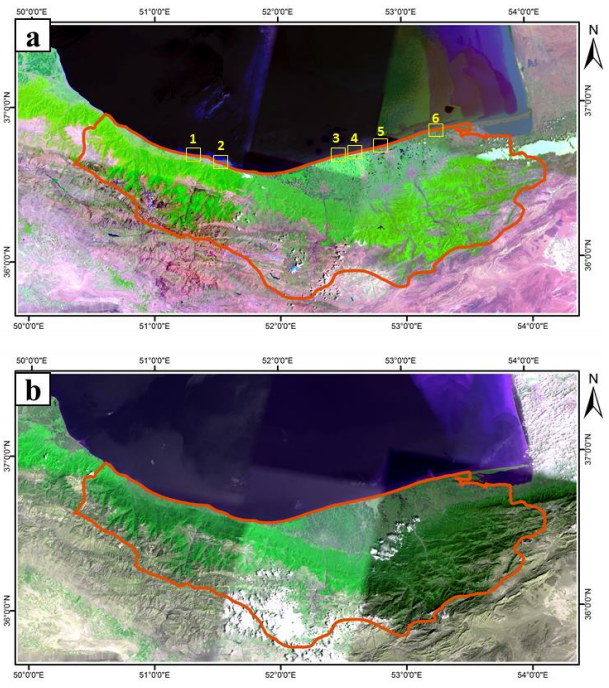

Figure 2. Color composite images of the study area; a) OLI bands of 7, 5 and 3 as RGB; yellow boxes show the location of main shore changes; b) TM bands 2, 3 and 1 as RGB.

2.3 GEE platform

GEE which hosts satellite imagery, is a web-based geospatial processing platform and service and makes satellite imagery available for data mining on a global scale. In the literature, various academic studies have been conducted on remote sensing using GEE (e.g., Gorelick et al., 2017; Kennedy et al., 2018; Mateo-García et al., 2018; Mutanga and Kumar, 2019; Arévalo et al., 2020; Ghorbanian et al., 2020; Wang et al., 2020; Cavdaroglu, 2021). The methodology adopted in this study in the GEE platform is illustrated in figure 3.

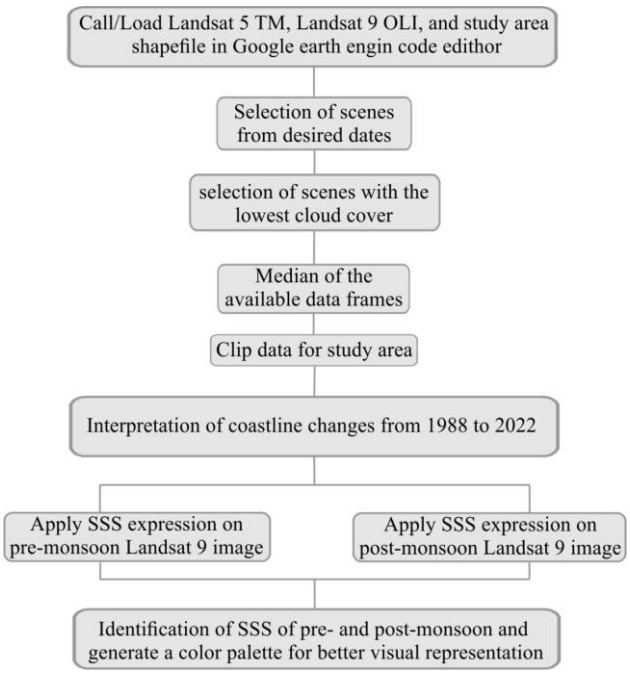

Figure 3. Methodology flow chart.

2.4 Shoreline Changes

shorelines have never been stable in either their long-term or short-term positions. shoreline change detection and mapping are critical for safe navigation, coastal resource management, coastal environmental protection and sustainable coastal development and planning (Lockwood, 1997; Shaw and Allen, 1995). Caspian Sea have very dynamic coastlines which are required to be monitored and mapped by rapid trustworthy techniques (Rasuly et al., 2010). The coastal zone features were delineated using Landsat 5 TM and Landsat 9 OLI data, respectively, from 1988 and 2022 (before the monsoon). Manual identification technique was used for coastline detection and extraction (Figure 4).

2.5 Sea Surface Salinity

Sea salinity is one of the prime environmental factors of sea water that affect the distribution of creatures in the sea. The amount of salinity changes with evaporation, precipitation, and surface water inflow (Sigman, and Hain, 2012). Researchers have developed linear and nonlinear algorithms to SSS using MODIS data (e.g., Geiger et al., 2013; Maged and Mazlan, 2009; Vogel and Brown, 2016; Xiang et al., 2017). However, there are limited study in using Landsat data for this purpose (e.g., Zhao et al., 2017; Bakir Bakir et al., 2020).

The median of Landsat 9 OLI images of the study area from May to June of 2022 was prepared for retrieving the SSS as the pre-monsoon dataset. The median of Landsat 9 OLI images of this region from July to August of 2022 was also prepared as the post-monsoon dataset. The logical operation algorithm which was proposed by Seenipandi et al. (2021) was applied and tested on the pre- and post-monsoon datasets for measuring the SSS in practical salinity unit (PSU) over the south coast of the Caspian Sea. 1 PSU is 1 gram of salt per 1000 gram of water. The following SSS expression was implemented on the datasets (eq. 1):

$$SSS = (14.256 - 240.163 * \text{Band } 4) - (72.533 * \text{Band } 5) + (124.700 * \text{Band } 2) + (191.266 * \text{Band } 3) + (36.044 * \text{Band } 9) - (11.117 * \text{Band } 6) - (39.789 * \text{Band } 7) \quad (1)$$

2.6 In-situ measurement

Measurement of sea salinity were taken at the selected sites in the Caspian Sea over a period of 4 days in August 2022, via boats along the Mazandaran coast in the same time as the satellite data of post-monsoon were collected (Figure 6). A total of 20 near shore sampling sites were selected for recording the SSS (Table 2).

3. RESULTS AND DISSCUSSION

3.1 Detection of Shoreline Changes

The advances of shoreline position were mainly detected over these 33 years in 6 points (figure 4), as a result of breakwaters, which are constructed to prevent erosion and the structural buildings such as recreational piers or wharves.

3.2 Satellite data derived SSS

The results showed that the SSS was within the estimated range of about 3–20 PSU (Figure 5). The higher range of SSS is spatially along the nearshore with a maximum of about 9-20 PSU in the pre-monsoon image (Figure 5a). It is due to the flow of water from the east that changes the salt content, which gradually decreases towards the sea and dilutes the salinity. The lower amount of SSS in some places nearshore as well as toward the sea is due to the mixing of freshwater from river discharge and probable precipitation. It is obvious in both pre-monsoon and post-monsoon images that the eastern shore of the Caspian Sea is more saline than the other parts. The reason is that the rate of precipitation gradually increases from the eastern coasts toward the west. However, the higher range of SSS in this part of the post-monsoon image is spatially developed and its salinity has been decreased (Figure 5b). The nearshore salinity in the post-monsoon image is lower than that of pre-monsoon that shows the significant role of the Indian monsoon rainfall.

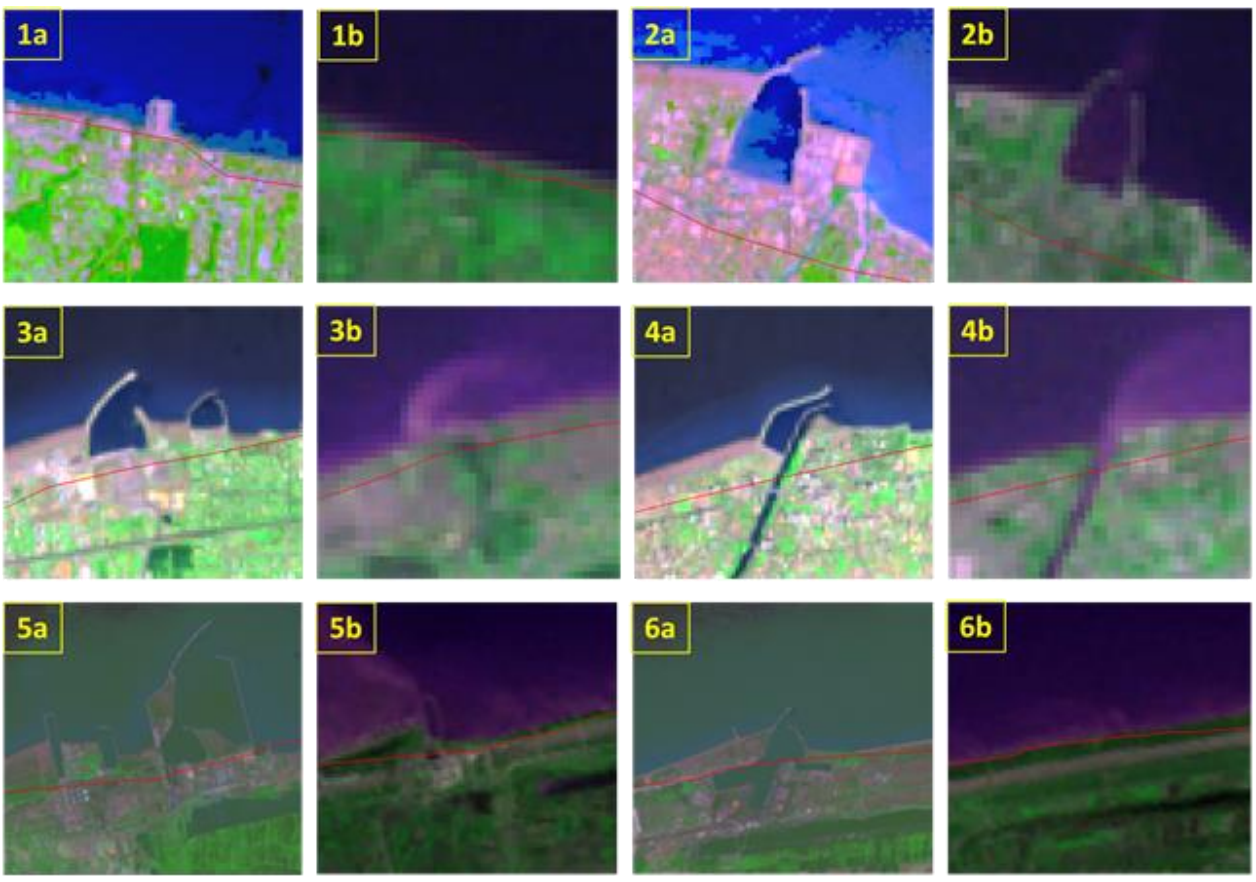

Figure 4. The main shoreline changes over 33 years in Mazandaran coastline. The numbers of each changes refer to the location boxes which are shown in Figure 1. The letter "a" indicates the shoreline increases in 2022, obtained from OLI data and the "b" letter is regarded to TM data from 1988.

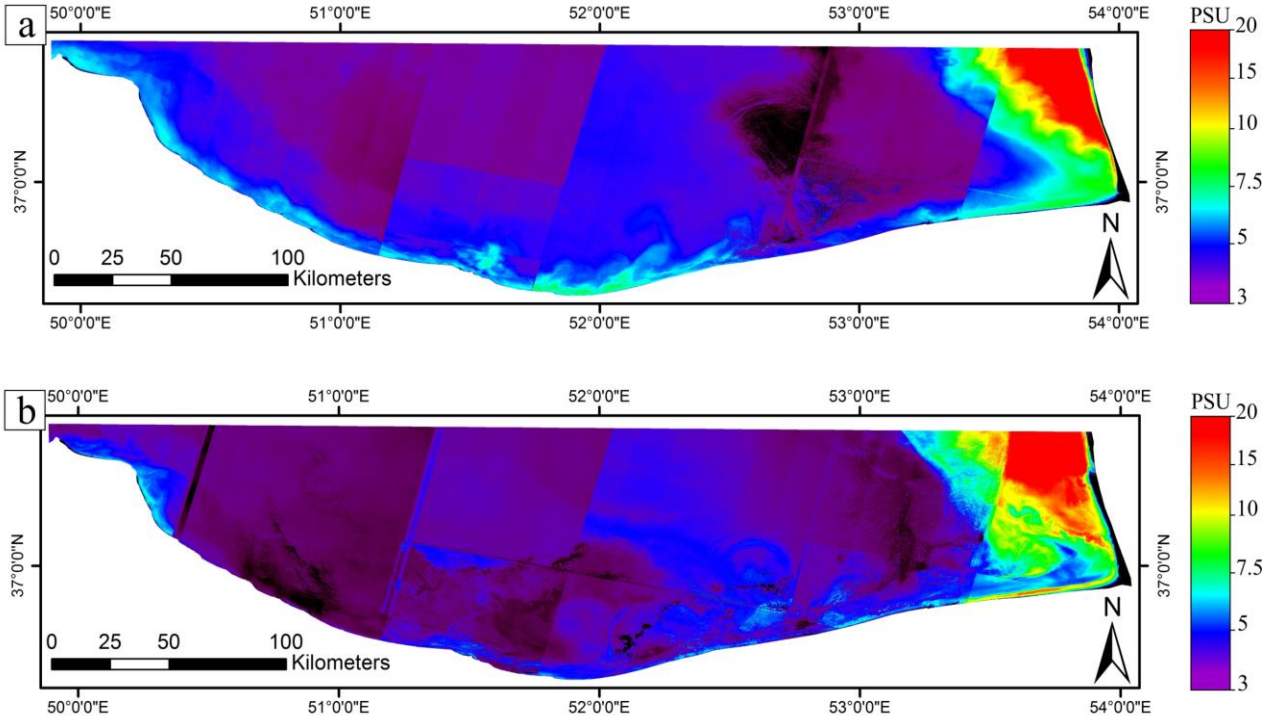

Figure 5. The sea surface salinity of the Caspian Sea obtained from Landsat 9 OLI data of pre-monsoon (a) and post-monsoon (b), summer 2022.

3.3 Accuracy assessments

The obtained SSS of post-monsoon from Landsat data was validated by in-situ measurements in 20 stations (Figure 6, Table 2). The value of R^2 was estimated 0.92, which indicates a strong correlation between observed and satellite-derived SSS product (Figure 7).

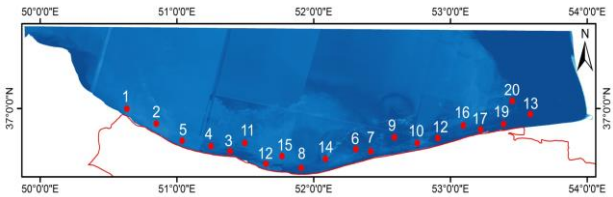

Figure 6. Locations of sampling stations in Mazandaran coastline during post-monsoon, August 2022.

Station No.	Near-Shore SSS	Station No.	Near-Shore SSS
1	3.02	11	4.79
2	2.89	12	8.56
3	7. 25	13	11.87
4	9. 65	14	5.01
5	5.95	15	4.86
6	13. 11	16	9.56
7	13.23	17	10.01
8	4.06	18	7.69
9	7. 86	19	15. 45
10	8.14	20	17.10

Table 2. In-situ SSS values (ppt) of Caspian Sea (August 2022, post monsoon period).

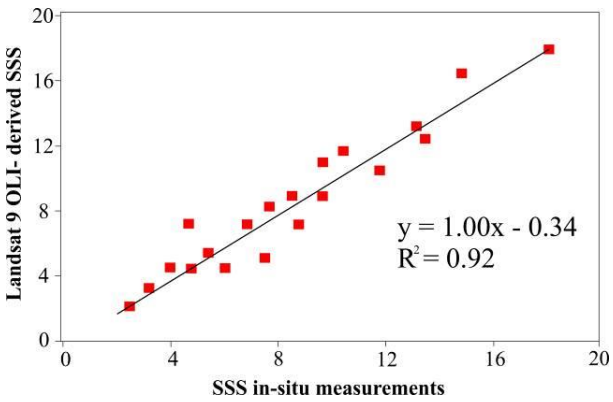

Figure 7. Value of SSS estimated from Landsat 9 OLI versus in-situ measurements.

4. CONCLUSIONS

This study showed that the rate of increase in the shoreline was more than decreasing through these years and the construction of a few breakwaters through the Mazandaran coast has relatively prevented coastal erosion. Coastal areas have always been a popular place for recreation, habitation, and commerce. Therefore, shoreline monitoring using high

spatial resolution sensors during short time intervals is essential for shoreline management.

The salinity of water body provides information about its formation source, and it is driven by the net influx of fresh water at the air-sea interface due to evaporation, precipitation, and river inflow. The applied method successfully determined the SSS in the Caspian Sea. As a result, it is suggested to use this method for the measurement of salinity during pre-monsoon, monsoon, and post-monsoon periods and the determination of seasonal SSS over the Caspian Sea. Furthermore, OLI-derived SSS can be compared to MODIS- derived SSS in future studies.

The GEE provides an open-source better platform to process, analyze and prepare an app for Near-Real-Time coastal monitoring. Such image processing and investigating imagery for this study area would take several days of a person's time using traditional methodologies. However, these basic operations require only 20-40 minutes when using the GEE platform, and new study areas can be simply added to the research by adding a few lines of code.

REFERENCES

Alizadeh, H., Naderi Beni, A., Tavakoli, V., 2018. Heavy metals in coastal sediments of South Caspian Sea: natural or anthropogenic source? *Caspian Journal of Environmental Sciences*, 16 (1), 45–61.

Arévalo, P, Bullock, E. L, Woodcock, C. E., Olofsson, P., 2020. A Suite of Tools for Continuous Land Change Monitoring in Google Earth Engine. *Front. Clim.*, 2, 576740.

Bakir, B., Zisykien, F. A., Umam, B. A., Munib, A., 2020. Salinity and Sulphate Concentration Mapping and Analysis: Sea Surface at the Madura Island Context. *IOP Conf. Ser.: Earth Environ. Sci.*, 469, 012105.

Cavdaroglu, G. C., 2021. Google Earth Engine Based Approach for Finding Fire Locations and Burned Areas in Muğla, Turkey. *American Journal of Remote Sensing*, 9 (2), 72-77.

Dassenakis, M., Paraskevopoulou, V., Cartalis, C., Adaktilou, N. and Katsiabani, K., 2012. Remote sensing in coastal water monitoring: Applications in the eastern Mediterranean Sea (IUPAC Technical Report). *Pure Appl. Chem.*, 84 (2), 335–375.

Geiger, F., Grossi, D., Trembanis, C., Kohut, T., Oliver, J., 2013. Satellite-derived coastal ocean and estuarine salinity in the Mid-Atlantic. *Cont. Shelf Res.*, 63, S235–S242.

Gorelick, N., Hancher, M., Dixon, M., Ilyushchenko, S., Thau, D., Moore, R., 2017. Google Earth Engine: Planetary-scale geospatial analysis for everyone. *Remote Sensing of Environment*, 202, 18-27.

Ghorbanian, A., Kakooei, M., Amani, M., Mahdavi, S., Mohammadzadeh, A., Hasanlou, M., 2020. Improved land cover map of Iran using Sentinel imagery within Google Earth Engine and a novel automatic workflow for land cover classification using migrated training samples. *ISPRS Journal of Photogrammetry and Remote Sensing*, 167, 276-288.

Jin, Q., Wei, J., Lau, W. K. M., Pu, B., Wang, C., 2021. Interactions of Asian mineral dust with Indian summer monsoon: Recent advances and challenges, *Earth-Science Reviews*, 215, 103562.

Kennedy, R. E., Yang, Z., Gorelick, N., Braaten, J., Cavalcante, L., Cohen, W. B., Healey, S., 2018. Implementation of the LandTrendr algorithm on google earth engine. *Remote Sensing*, 10 (5), 691.

Khaleghizavareh, H., 2005. Climate comfort classification in southern coastal area of Caspian Sea. *Proc International Conference on Rapid Sea-Level Change: a Caspian Perspective*, pp. 2–9.

Lockwood, M., 1997. *NDSI shoreline briefing to the FGDC Coordinate group*. NOAA/NOS.

Maged, M., Mazlan, H., 2009. Linear algorithm for salinity distribution modeling from MODIS data. *In CD-ROM Proceeding of IGARSS*.; Cape Town University: Cape Town, South Africa, 12–17.

Mateo-García, G., Gómez-Chova, L., Amorós-López, J., Muñoz-Marí, J., Camps-Valls, G., 2018. Multitemporal cloud masking in the Google Earth Engine. *Remote Sensing*, 10 (7), 1079.

Mutanga, O., Kumar, L., 2019. Google earth engine applications. *Remote Sensing*, 11 (5), 591.

Palacios, S., Peterson, T.D., Kudela, R., 2009. Development of synthetic salinity from remote sensing for the Columbia River Plume. *J. Geophys. Res. Ocean*, 114.

Qing, S., Zhang, J., Cui, T., Bao, Y., 2013. Retrieval of sea surface salinity with MERIS and MODIS data in the Bohai Sea. *Remote Sensing of Environment*, 136, 117–125.

Rasuly, A.A., Naghdifar, R., Rasoli, M., 2010. Monitoring of Caspian Sea Coastline Changes Using Object-Oriented Techniques. *Procedia Environmental Sciences*, 2, 416-426.

Seenipandi, K., Ramachandran, K.K., Ghadei, P., Shekhar, S., 2021. Ocean remote sensing of seawater salinity and its seasonal variability: a case study of Southern Indian coastal water using Landsat 8 OLI images. *Remote Sensing of Ocean and Coastal Environments, Earth Observation*, 65-81.

Shaw, B., Allen, J.R., 1995. Analysis of a dynamic shoreline at Sandy Hook. New Jersey, using a GIS. *Proceedings of ASPRS/ACSM 1995*, 382-391.

Sigman, D., Hain, M., 2012. The Biological Productivity of the Ocean. *Nature Education*, 3,1-16.

Vogel, R., Brown, C., 2016. Assessing satellite sea surface salinity from ocean color radiometric measurements for coastal hydrodynamic model data assimilation. *J. Appl. Remote Sens.*, 10, 036003.

Wang, L., Diao, C., Xian, G., Yin, D., Lu, Y., Zou, S., Erickson, T. A., 2020. A summary of the special issue on

remote sensing of land change science with Google earth engine. *Remote Sensing of Environment*, 248, 112002.

Webster, P. J., Magaña, V. O., Palmer, T. N., Shukla, J., Tomas, R. A., Yanai, M., Yasunari, T., 1998. Monsoons: Processes, predictability, and the prospects for prediction. *J. Geophys. Res. Oceans*, 103, 14451–14510.

Xiang, Y.; Bei, X.; Xiangyang, Y.; Yebao, L.; Buli, W.; Cui, B.; Xin, L. Retrieval of remotely sensed sea surface salinity using MODIS data in the Chinese Bohai Sea. *Int. J. Remote Sens.*, 38, 7357–7373.

Zhao, J., Temimi, M., Ghedira, H., 2017. Remotely sensed sea surface salinity in the hyper-saline Arabian Gulf: Application to landsat 8 OLI data. *Estuarine, Coastal and Shelf Science*, 187, 168-177.